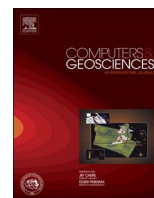




ELSEVIER

Contents lists available at ScienceDirect

Computers & Geosciences

journal homepage: www.elsevier.com/locate/cageo

Case study

A visualization tool for the kernel-driven model with improved ability in data analysis and kernel assessment

Yadong Dong^a, Ziti Jiao^{a,b,*}, Hu Zhang^{c,d}, Dongni Bai^a, Xiaoning Zhang^a, Yang Li^a, Dandan He^a^a State Key Laboratory of Remote Sensing Science and School of Geography, Beijing Normal University, Beijing 100875, China^b Beijing Key Laboratory of Environmental Remote Sensing and Digital City, Beijing Normal University, Beijing 100875, China^c College of Urban and Environmental Sciences, Tianjin Normal University, Tianjin, China^d Tianjin Engineering Centre for Geospatial Information Technology, Tianjin, China

ARTICLE INFO

Article history:

Received 10 March 2016

Accepted 8 June 2016

Available online 11 June 2016

Keywords:

Kernel-driven model

Interactive data language

Bidirectional reflectance distribution function

Albedo

Visualization tool

ABSTRACT

The semi-empirical, kernel-driven Bidirectional Reflectance Distribution Function (BRDF) model has been widely used for many aspects of remote sensing. With the development of the kernel-driven model, there is a need to further assess the performance of newly developed kernels. The use of visualization tools can facilitate the analysis of model results and the assessment of newly developed kernels. However, the current version of the kernel-driven model does not contain a visualization function. In this study, a user-friendly visualization tool, named MaKeMAT, was developed specifically for the kernel-driven model. The POLDER-3 and CAR BRDF datasets were used to demonstrate the applicability of MaKeMAT. The visualization of inputted multi-angle measurements enhances understanding of multi-angle measurements and allows the choice of measurements with good representativeness. The visualization of modeling results facilitates the assessment of newly developed kernels. The study shows that the visualization tool MaKeMAT can promote the widespread application of the kernel-driven model.

© 2016 Elsevier Ltd. All rights reserved.

1. Introduction

Bidirectional Reflectance Distribution Function (BRDF) models for correcting bidirectional reflectance can be applied in many applications of quantitative remote sensing. Among the available BRDF models, semi-empirical kernel-driven models are considered to be some of the most versatile and the easiest to implement. Such models have the advantage of being able to adjust to many different kinds of land surface types and can be inverted analytically (Gao et al., 2001).

The basic concept of the semi-empirical kernel-driven model was first introduced by Roujean et al. (1992) and was further developed by Wanner et al. (1995) and Lucht et al. (2000). To make the kernel-driven model easier to understand and use, a research-grade modeling framework for the kernel-driven model, named AMBRALS, was provided by Wanner for the user community (Wanner et al., 1995, 1997, Lucht et al., 2000). A new kernel known as LiTransit was developed by Li et al. (1999) to improve the extrapolation ability under large zenith angles. The model was

further developed by Maignan et al. (2004) and Jiao et al. (2013) to improve its hotspot effect. A new inversion method was developed by Jiao et al. (2014) that is able to utilize prior knowledge to obtain increased accuracy when the number of multi-angle measurements is insufficient.

The semi-empirical kernel-driven model has been widely used in many aspects of remote sensing. The model is used (1) to produce BRDF/Albedo products from spaceborne sensors, such as Moderate Resolution Imaging Spectroradiometer (MODIS) (Lucht et al., 2000; Schaaf et al., 2002), the Polarization and Directionality of the Earth's Reflectances (POLDER) (Deschamps et al., 1994; Bicheron and Leroy, 2000; Bacour and Bréon, 2005), and the Meteosat Second Generation (MSG) (Van Leeuwen and Roujean, 2002); (2) to retrieve vegetation structure parameters, such as Clumping Index (CI) and Leaf Area Index (LAI) (Chopping et al., 2008; Hill et al., 2011; Wang et al., 2011; He et al., 2012; Zhu et al., 2012; He et al., 2016); (3) to classify and map land cover (Friedl et al., 2002, 2010; Zhang et al., 2003; Jiao et al., 2011; Jiao and Li, 2012); (4) to couple surface reflectance with atmospheric scattering to achieve improved atmospheric correction (Leroy and Roujean, 1994; Wu et al., 1995; Wang et al., 2010; Litvinov et al., 2011); (5) to accumulate and apply prior knowledge of BRDF archetypical shapes (Jiao et al., 2014, 2015; Zhang et al., 2015; Li et al., 2001); and (6) to correct surface reflectance bidirectionality

* Correspondence to: Beijing Normal University, No. 19, Xijiekouwai Street, Haidian District, Beijing 100875, China.

E-mail address: jiaozt@bnu.edu.cn (Z. Jiao).

(Roujean et al., 1992; Leroy and Roujean, 1994). Nonetheless, the widespread application of the kernel-driven model may be hindered as a result of various issues.

With the development of the kernel-driven model, many new kernels have been introduced (Roujean et al., 1992; Wanner et al., 1995; Li et al., 1999; Lucht et al., 2000; Maignan et al., 2004; Jiao et al., 2013). Currently available kernels in the kernel-driven model include 6 volume-scattering kernels and 7 geometric-optical kernels. These kernels can be used to form 42 unique types of models, with additional model types possible if more kernels are developed. It is difficult for users with little background knowledge in these kernels to choose the best-fitted kernel combinations to achieve the ideal result. Therefore, there is a need to help users understand the differences among different kernel combinations and assess newly developed kernels.

AMBRALS, the current software for the kernel-driven model for the user community, is written in the C programming language (Wanner et al., 1995, 1997; Lucht et al., 2000). AMBRALS is manipulated via Command Line Interface (CLI), and the results are provided in a text file. This condition may hinder the widespread application of the kernel-driven model (Moeck et al., 2015). Therefore, the user interaction aspect of the kernel-driven model should be improved.

Here, we contribute to fulfilling these needs by presenting a visualization tool for the kernel-driven model, named MaKeMAT. In MaKeMAT, newly developed kernels can be easily added, and users can learn the differences among different kernel combinations and assess the accuracy of newly developed kernels.

2. Kernel-driven model

The equation for the kernel-driven model was given by Roujean et al. (1992):

$$R(\theta_i, \theta_v, \phi, \Lambda) = f_{iso}(\Lambda) + f_{vol}(\Lambda)K_{vol}(\theta_i, \theta_v, \phi) + f_{geo}(\Lambda)K_{geo}(\theta_i, \theta_v, \phi) \quad (1)$$

where $R(\theta_i, \theta_v, \Phi, \Lambda)$ is the BRDF in band Λ ; $K_{vol}(\theta_i, \theta_v, \Phi)$ and $K_{geo}(\theta_i, \theta_v, \Phi)$ are the volumetric scattering kernels and geometric-optical surface scattering kernels, respectively, which are functions of the solar zenith angle (θ_i), view zenith angle (θ_v) and relative azimuth angle (Φ); and f_{iso} , f_{vol} and f_{geo} are the weight coefficients of the corresponding kernels. The optimal weight coefficients can be retrieved using the least-square method. Reflectance in any illumination and view direction can then be retrieved using these weight coefficients.

The integral of the kernel can be calculated in advance because the integral has little correlation with the coefficients to be retrieved. In addition, the white-sky albedo and black-sky albedo can be calculated using the weighted sum of the integrals of three kernels (Lucht et al., 2000).

The efficiency of the model is determined by the volume-scattering and geometric-optical kernels. The equations for the available volume-scattering and geometric-optical kernels are introduced below.

2.1. Volume-scattering kernels

The volume-scattering kernels are based on the radiative transfer theory presented by Ross (1981). The kernels include the Rossthick (Roujean et al., 1992), Rossthin (Wanner et al., 1995), RossthickMaignan (Maignan et al., 2004), and RossthickChen kernels (Jiao et al., 2013).

The Rossthick kernel was derived by Roujean et al. (1992) based on the radiative transfer theory of Ross (1981) with the following

equation:

$$K_{Rossthick} = \frac{(\frac{\pi}{2} - \xi)\cos \xi + \sin \xi}{\cos \theta_i + \cos \theta_v} - \frac{\pi}{4} \quad (2)$$

where ξ is the phase angle, which satisfies

$$\cos \xi = \cos \theta_i \cos \theta_v + \sin \theta_i \sin \theta_v \cos \phi \quad (3)$$

The Rossthin kernel was derived by Wanner et al. (1995) based on a small LAI approximation with the following equation:

$$K_{Rossthin} = \frac{(\frac{\pi}{2} - \xi)\cos \xi + \sin \xi}{\cos \theta_i \cos \theta_v} - \frac{\pi}{2} \quad (4)$$

Maignan et al. (2004) added a hotspot factor derived by Bréon et al. (2002) based on the mutual shadowing theory by Jupp and Strahler (1991) to generate the so-called RossthickMaignan (RTM) kernel (Maignan et al., 2004). The equation for the RTM kernel is

$$K_{RTM} = \frac{(\frac{\pi}{2} - \xi)\cos \xi + \sin \xi}{\cos \theta_i + \cos \theta_v} \times \left[1 + C_h \left(1 + \frac{\xi}{\xi_0} \right)^{-1} \right] - \frac{\pi}{4} \quad (5)$$

where ξ_0 is a characteristic angle that characterizes the width of the hotspot. Most values of ξ_0 were in the range 1–2°, and ξ_0 was set as a constant value of 1.5° to avoid the addition of a free parameter in the kernel-driven model (Maignan et al., 2004). Notably we add a parameter C_h to characterize the height of the hotspot.

Jiao et al. (2013) added a hotspot factor derived by Chen and Cihlar (1997) to the Rossthick kernel to generate the so-called RossthickChen (RTC) kernel (Jiao et al., 2013; Jiao et al., in press). The equation for the RTC kernel is

$$K_{RTC} = \frac{(\frac{\pi}{2} - \xi)\cos \xi + \sin \xi}{\cos \theta_i + \cos \theta_v} \times \left(1 + C_1 e^{-\frac{\xi}{C_2}} \right) - \frac{\pi}{4} \quad (6)$$

where $1 + C_1 e^{-\frac{\xi}{C_2}}$ is the hotspot function with two adjustable parameters C_1 and C_2 for analyzing the possible variation in hotspot height and width in fitting hotspot BRDFs. The kernel significantly improves the accuracy in estimating the hotspot reflectance (Jiao et al., 2013).

Fig. 1 presents the shapes of the above-mentioned volume-scattering kernels. All graphics in Fig. 1 are produced by MaKeMAT.

2.2. Geometric-optical kernels

The geometric-optical kernels include the Roujean kernel (Roujean et al., 1992), LiSparse and LiDense kernel (Wanner et al., 1995), LiTransit kernel (Li et al., 1999) and reciprocal versions of the Li kernels (Lucht et al., 2000).

The Roujean kernel was derived by Roujean et al. (1992) with the following equation:

$$K_{Roujean} = \frac{1}{2\pi} [(\pi - \phi)\cos \phi + \sin \phi] \tan \theta_i \tan \theta_v - \frac{1}{\pi} \left(\tan \theta_i + \tan \theta_v + \sqrt{\tan^2 \theta_i + \tan^2 \theta_v - 2 \tan \theta_i \tan \theta_v \cos \phi} \right) \quad (7)$$

There is only one weak hotspot in the Roujean kernel because it does not consider the overlap of the shadows.

The LiSparse kernel was derived from the geometric-optical, mutual-shadowing BRDF model by Li and Strahler (1992) with the following equation (Wanner et al., 1995):

$$K_{LiSparse} = O(\theta'_i, \theta'_v, t) - \sec \theta'_i - \sec \theta'_v + \frac{1}{2} (1 + \cos \xi') \sec \theta'_i \quad (8)$$

where

دانلود مقاله



<http://daneshyari.com/article/506785>



- ✓ امکان دانلود نسخه تمام متن مقالات انگلیسی
- ✓ امکان دانلود نسخه ترجمه شده مقالات
- ✓ پذیرش سفارش ترجمه تخصصی
- ✓ امکان جستجو در آرشیو جامعی از صدها موضوع و هزاران مقاله
- ✓ امکان پرداخت اینترنتی با کلیه کارت های عضو شتاب
- ✓ دانلود فوری مقاله پس از پرداخت آنلاین
- ✓ پشتیبانی کامل خرید با بهره مندی از سیستم هوشمند رهگیری سفارشات